An experimental and theoretical investigation into positron and electron scattering from formaldehyde

J. Phys. B: At. Mol. Opt. Phys. **44** (2011) 195202 (8pp) doi:10.1088/0953-4075/44/19/195202

An experimental and theoretical investigation into positron and electron scattering from formaldehyde

A Zecca[1], E Trainotti[1], L Chiari[1,2], G García[3], F Blanco[4], M H F Bettega[5], M T do N Varella[6], M A P Lima[7] and M J Brunger[2,8]

[1] Department of Physics, University of Trento, Povo, I-38123 Trento, Italy
[2] ARC Centre for Antimatter-Matter Studies, School of Chemical and Physical Sciences, Flinders University, GPO Box 2100, Adelaide, South Australia 5001, Australia
[3] Instituto de Matemáticas y Física Fundamental, CSIC, Serrano 121, 28006 Madrid, Spain
[4] Facultad de Ciencias Físicas, Departamento de Física Atómica, Molecular y Nuclear, Universidad Complutense, Avda. Complutense s/n, E-28040 Madrid, Spain
[5] Departamento de Física, Universidade Federal do Paraná, Caixa Postal 19044, 81531-990 Curitiba, Paraná, Brazil
[6] Instituto de Física, Universidade de São Paulo, Caixa Postal 66318, 05315-970 São Paulo, SP, Brazil
[7] Instituto de Física 'Gleb Wataghin', Universidade Estadual de Campinas, Caixa Postal 6165, 13083-970 Campinas, São Paulo, Brazil; Laboratório Nacional de Ciência e Tecnologia do Bioetanol (CTBE), Centro Nacional de Pesquisa em Energia e Materiais (CNPEM), Caixa Postal 6170, 13083-970 Campinas, São Paulo, Brazil
[8] Institute of Mathematical Sciences, University of Malaya, 50603 Kuala Lumpur, Malaysia

E-mail: Michael.Brunger@flinders.edu.au

Received 11 July 2011, in final form 11 August 2011
Published 2 September 2011
Online at stacks.iop.org/JPhysB/44/195202

Abstract
We report on measurements of total cross sections (TCSs) for positron scattering from the fundamental organic molecule formaldehyde (CH_2O). The energy range of these measurements was 0.26–50.3 eV, whereas the energy resolution was ~260 meV. To assist us in interpreting these data, Schwinger multichannel level calculations for positron elastic scattering from CH_2O were also undertaken (0.5–50 eV). These calculations, incorporating an accurate model for the target polarization, are found to be in good qualitative agreement with our measured data. In addition, in order to compare the behaviour of positron and electron scattering from this species, independent atom model-screened additivity rule theoretical electron TCSs, now for energies in the range 1–10 000 eV, are also reported.

(Some figures in this article are in colour only in the electronic version)

1. Introduction

We have recently been focussing our attention on the experimental study of positron scattering from biomolecules [2–7], in order to provide total cross section (TCS) data for scientists seeking to simulate the tracks of charged particles as they move through matter [8, 9] and to study the behaviour of positron swarm transport in various gases [10, 11]. Note that in the former case, TCSs are important as they specify the mean free path between collisions in such studies. While these investigations are certainly in an area of current topical interest, we should not forget that providing accurate and reliable TCS measurements, to assist in the development of positron scattering theory, remains an important avenue of research. For example, in an earlier joint study on formic acid [12], we were able to elucidate, by comparing various levels of theory with experiment, the main interactions that contributed to the scattering dynamics (target polarization and the target permanent dipole moment). Agreement in terms of the absolute magnitude of the experimental and theoretical cross sections, however, remained qualitative suggesting that

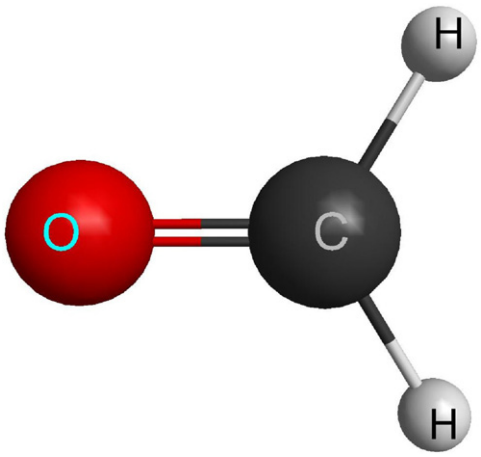

Figure 1. Geometric structure of the CH_2O molecule (generated using McMolPlt [1]).

some further development in either the experimental method or in the scattering model was required.

Formaldehyde (CH_2O) is an excellent candidate species on which to benchmark further theoretical developments. It is a relatively small system and is the simplest compound containing the important carbonyl functional group (see figure 1), which is responsible for its strong dipolar nature. Formaldehyde also possesses a strong permanent dipole moment of value 2.43 D [13] and an average dipole polarizability ($\overline{\alpha}$ = 16.53 au [14]) of intermediate magnitude. In spite of these interesting intrinsic physico-chemical properties, we can find no previous experimental or theoretical investigations into positron-CH_2O scattering suggesting that the current work is original. From the electron scattering perspective, the situation is better, although most of the available absolute cross section results are theoretical (see [15, 16] and [17], and references therein) with the experimental studies being relative and largely concentrating on the vibrational and electronic-state spectroscopy (see e.g. [18, 19]). The exception to this is a couple of absolute vibrational excitation functions (at a scattering angle of 90°) from Kato *et al* [20]. Surprisingly, we can find no experimental TCSs for electron-CH_2O scattering. As a consequence of the above summary, we believe that the present investigation, incorporating both theory and experiment for positrons and theory for electrons, is timely.

In the next section, we give a summary of our experimental apparatus and techniques. Thereafter, in section 3, we provide details of our electron-independent atom model-screened additivity rule (IAM-SCAR) method and our positron Schwinger multichannel (SMC) level calculations. In section 4, we report the present results and provide a discussion of those results, before drawing some conclusions from our investigation.

2. Experimental details

The positron spectrometer at the University of Trento was developed by Zecca and has been described in some detail recently [21]. We therefore do not need to repeat those details here, except for noting that a tungsten moderator of thickness 1 μm [22] was employed in conjunction with a radioactive ^{22}Na isotope (current activity ∼1.6 mCi) and some electrostatic optics in order to produce the positron beam. Note that in our laboratory, as a check for the validity of our techniques and procedures, we carry out initial validation measurements using targets for which the positron scattering TCSs might be considered to be well known. Such systems might be drawn from molecular nitrogen [21] or from the rare gases [23, 24].

The basis of all linear transmission measurements is the Beer–Lambert law, as defined by

$$I_1 = I_0 \exp\left(\frac{-(P_1 - P_0)L\sigma}{kT}\right), \qquad (1)$$

where I_1 is the positron beam count rate at pressure P_1, the target pressure being measured with the CH_2O routed to the scattering cell, k is Boltzmann's constant (1.38×10^{-23} JK^{-1}) and T is the temperature of the CH_2O vapour (K), as accurately measured using a calibrated platinum (PT100) resistance thermometer that is in excellent thermal contact with the scattering chamber. In our geometry, gas molecules thermalize with the scattering cell walls; therefore, the scattering chamber temperature can be viewed as a good approximation of the gas temperature. σ is the TCS of interest at a given positron energy (E); I_0 is the positron count rate at P_0, the pressure with CH_2O diverted into the vacuum chamber, i.e. away from the scattering cell; and L is the length of the scattering region.

For a valid application of equation (1), several crucial precautions should be taken and care must be exercised during the measurements. These considerations include minimizing the double-scattering events and ensuring that the TCSs are independent of pressure. In this work, high purity paraformaldehyde ($OH(CH_2O)_nH$, with n = 8–100), which is a non-volatile solid polymer at room temperature, was gently dry heated to ∼60 ± 1 °C in order to be depolymerized and produce a stable and pure (∼99%) source of formaldehyde gas for the scattering experiments. Note that at this temperature the vapour pressure of paraformaldehyde is orders of magnitude (∼2000 times) smaller than that of formaldehyde [25], with a typical formaldehyde pressure of 10^{-3} torr being employed in our measurements. The vapour pressure of any molecular dissociation products is also known to be negligible [25].

The geometrical length of the scattering region is 22.1 ± 0.1 mm, with apertures of 1.5 mm diameter at both the entrance and exit of the scattering cell. As in our previous experiments, a further aperture of diameter 2 mm is placed 8 mm downstream of the scattering cell. This aperture has a twofold function: as a skimmer-like diaphragm, it reduces the gas pressure at the channeltron detector. In addition, it reduces the angular acceptance of the detector, thus reducing somewhat the angular resolution effect on the TCS measurements. End effects were minimized in this configuration by having equal and relatively small diameter entrance and exit apertures in our scattering cell. As a consequence, we evaluate that their contribution to the uncertainty in the value of L is less than 0.2%. In our application of equation (1), the value of L used is always corrected to account for the path increase caused by

the gyration of the positrons in the focusing axial magnetic field present in the scattering region. For E up to 35.3 eV, $B \sim 11$ G and the value of L increased by ∼5.5%, whereas for E between 35.3 and 50.3 eV, $B \sim 4$ G, leading to an increase in L of ∼2%. From a consideration of the size of the entrance and exit apertures of our scattering cell, and their separation, and the skimmer, the angular acceptance ($\Delta\theta$) of the Trento spectrometer is no worse than ≈4°, which compares favourably with that from the Detroit apparatus [26] ($\Delta\theta \approx 16°$). The gyration of the positrons can also potentially increase the angular resolution error compared with the no-field case [27]. Using some of the analytic formulae detailed in Kauppila *et al* [26], but for our conditions, estimates of the energy-dependent angular discrimination can be obtained. We found that they varied from ∼17° at 1 eV positron energy to ∼5.4° at 10 eV. This can be corrected for, provided absolute elastic differential cross sections (DCSs) are available [28]. In principle, such DCSs are available from our SMC level calculations. However, as we shall see later in our results and discussion section, at this time employing those DCS in this manner might be a little premature and so we have not done so. As a consequence, the TCSs we report here represent a lower bound on the exact values.

It is crucial that the energy scale be calibrated accurately. The zero for the energy scale, in the absence of the target gas, was determined in this investigation using a retarding potential analysis of the positron beam [29]. We now believe that the error in our energy scale is ±0.1 eV. Measurements carried out during the last four–five years show a surprising stability in the energy zero (variance <0.05 eV) when using the tungsten moderator. The same measurements allow us to evaluate the energy width of our positron beam as ∼260 meV, with an uncertainty in this determination of at most ±50 meV. It is also very important to accurately measure the scattering cell pressure, which we achieve with a MKS 627B capacitance manometer operating at 45 °C. As the manometer temperature was different from that of the target gas in the scattering cell, thermal transpiration corrections to the pressure readings are made using the approach of Takaishi and Sensui [30]. Typically, this led to a maximum correction on the TCS of +3%. One final caveat on the data we report should be noted. All of the experimental data are convoluted with the finite energy resolution of our positron beam, although the effect of this on the measured TCSs is most manifest at positron energies below ∼0.5 eV, which coincides with the energies where the slope of the TCS as a function of energy is also greatest. In practice, this physically implies that, when corrected for this effect, our lowest energy TCSs should be somewhat higher than we present here.

Finally, we note that the data collection and analysis codes were driven by software developed at the University of Trento, for application on a personal computer. The positron energy range of the present TCS measurements was 0.26–50.3 eV, with the overall errors on our TCSs estimated as being within the 5–15% range. Note that the overall errors are formed from the quadrature sum of quantities such as the statistical uncertainties on our data (see table 1), the uncertainty in our thermal transpiration corrections, the uncertainty in the value of L and the uncertainty in the absolute pressure readings (∼0.3%), as per the manufacturer's specifications. All of our measurements were taken under stable positron beam conditions.

Table 1. The present experimental TCSs ($\times 10^{-20}$ m^2) for positron scattering from formaldehyde (CH_2O). The uncertainties cited are purely statistical and are at the one standard deviation level.

Energy (eV)	TCS (10^{-20} m^2)	TCS error (10^{-20} m^2) ($\pm 1\sigma$)	Energy (eV)	TCS (10^{-20} m^2)	TCS error (10^{-20} m^2) ($\pm 1\sigma$)
0.26	253.8	32.5	4.50	24.2	0.3
0.30	246.9	25.8	4.75	23.5	0.9
0.35	213.2	23.9	5.00	21.8	0.2
0.40	195.1	19.2	5.3	22.2	0.3
0.45	162.7	14.5	5.8	19.9	0.9
0.55	148.8	7.9	6.3	19.1	0.1
0.65	120.7	4.8	6.8	18.0	1.8
0.75	109.6	4.0	7.3	17.0	0.5
0.95	87.3	3.0	8.3	16.4	0.4
1.05	80.2	3.5	9.3	16.5	0.6
1.25	65.5	2.9	10.3	15.2	0.5
1.50	54.6	1.7	12.8	14.7	0.8
1.75	49.6	1.8	15.3	14.2	0.4
2.00	45.2	1.7	17.8	13.5	0.5
2.25	39.8	2.4	20.3	13.2	0.4
2.50	35.9	0.9	22.3	13.1	0.4
2.75	34.1	1.3	25.3	12.6	0.7
3.00	31.1	1.6	27.3	12.5	0.5
3.25	29.8	0.8	30.3	12.0	0.5
3.50	28.2	0.2	35.3	12.4	1.0
3.75	26.2	1.3	40.3	11.7	0.3
4.00	25.3	0.3	45.3	12.0	0.8
4.25	24.7	1.2	50.3	12.2	0.4

3. Theoretical details

3.1. Electron scattering: the IAM-SCAR method

We have recently described [7] in some detail our IAM-SCAR approach to electron-polyatomic molecule scattering calculations, and so we do not repeat those details again here. Briefly, however, the first subjects of the present calculations are the atoms constituting formaldehyde, namely C, H and O. Our atomic optical model approach is essentially a potential scattering approach, in which (using atomic units with k^2 denoting the energy in Rydbergs) we solve the partial wave equation

$$\left(\frac{\mathrm{d}^2}{\mathrm{d}r^2} - \frac{\ell(\ell+1)}{r^2} - 2V_{\mathrm{mp}}(k,r)\right) U_\ell(k,r) = k^2 U_\ell(k,r), \tag{2}$$

where the local model potential is taken as

$$V_{\mathrm{mp}}(k,r) = V_{\mathrm{st}}(r) + V_{\mathrm{ex}}(k,r) + V_{\mathrm{pol}}(r) + \mathrm{i}V_{\mathrm{abs}}(k,r)\,. \tag{3}$$

Here $V_{\mathrm{st}}(r)$ is the standard Hartree potential of the target. It is then supplemented by the exchange potential $V_{\mathrm{ex}}(k,r)$ used by Riley and Truhlar [31], the polarization potential $V_{\mathrm{pol}}(r)$ employed by Zhang *et al* [32] and finally the imaginary absorption potential $\mathrm{i}V_{\mathrm{abs}}(k,r)$ of Staszewska *et al* [33]. Due to the imaginary absorption potential, the optical model

potential method yields a complex phase shift $\delta_\ell = \lambda_\ell + i\mu_\ell$. This allows for the calculation of cross sections (differential and integral) for elastic scattering, inelastic scattering (all excited and ionized states combined together) and the grand total as the sum of the integral cross sections (ICSs) of the two processes. A recent study of elastic electron scattering from atomic-iodine [34] showed the efficacy of this approach, as its results, except at the lowest energies (<3 eV), were found to be in very good accord with those from a fully *ab initio* and relativistic Dirac B-spline *R*-matrix method.

To now calculate the cross sections for electron scattering from CH_2O, we follow the independent atom method (IAM) by applying what is commonly known as the additivity rule (AR). In this approach, the molecular scattering amplitude is derived from the sum of all the relevant atomic amplitudes, including the phase coefficients, which leads to the molecular DCSs for the molecule in question. ICSs can then be determined by integrating those DCSs, with the sum of the elastic ICSs and absorption ICSs (now for all inelastic processes except rotations and vibrations) then giving the TCSs. A limitation of the AR is that no molecular structure is considered, so that it is really only applicable when the incident electrons are so fast that they effectively 'see' the target molecule as a sum of the individual atoms (typically above ∼100 eV). To reduce this limitation, García and colleagues [35, 36] introduced the screened additivity rule (SCAR) method, which considers the geometry of the relevant molecule (atomic positions and bond lengths) by using some screening coefficients. With this correction the range of validity might be extended to incident electron energies of 50 eV or a little lower. Furthermore, for polar molecules such as CH_2O, additional dipole-excitation cross sections can be calculated to extend the range of validity (∼20 eV). In the present implementation, rotational excitation cross sections for a free electric dipole are calculated by assuming that the energy transferred is low enough, compared to the incident energy, to validate the first Born approximation (FBA). Under these circumstances, we have calculated a rotational cross section for $J \rightarrow J'$ for CH_2O at 300 K by weighting the population for the Jth rotational quantum number at that temperature and estimating the average excitation energy from the corresponding rotational constants.

The results from applying the above approach are summarized in table 2. We note that the efficacy of the IAM-SCAR + dipole method, as applied to electron scattering from polar polyatomic molecules, at least down to energies of 20 eV, was recently demonstrated for elastic scattering from iodomethane by Hargreaves *et al* [37].

Table 2. The present calculated TCSs ($\times 10^{-20}$ m^2) for electron scattering from formaldehyde, using our IAM-SCAR + dipole correction method.

Energy (eV)	IAM-SCAR + dipole TCSs
1	160.18
1.5	114.53
2	90.45
3	66.37
4	54.89
5	47.60
7	38.64
10	31.08
15	25.79
20	23.02
30	19.80
40	17.64
50	15.99
70	13.67
100	11.45
150	9.24
200	7.87
300	6.16
400	5.12
500	4.42
700	3.47
1000	2.69
2000	1.55
3000	1.10
5000	0.71
10 000	0.38

3.2. Positron scattering: SMC method

The scattering cross sections were computed with the SMC method as implemented for collisions of positrons with molecules. The SMC method has been described in detail in several publications [38–41] and here we will only discuss those points that are relevant to the present calculations.

The SMC method is a variational method to calculate the scattering amplitude. The final expression to the scattering amplitude in the molecular reference frame (body-frame, BF) is

$$f(\vec{k}_f, \vec{k}_i) = -\frac{1}{2\pi} \sum_{m,n} \langle S_{\vec{k}_f} | V | \chi_m \rangle (d^{-1})_{mn} \langle \chi_n | V | S_{\vec{k}_i} \rangle, \quad (4)$$

where

$$d_{mn} = \langle \chi_m | A^{(+)} | \chi_n \rangle \quad (5)$$

and

$$A^{(+)} = Q\hat{H}Q + PVP - VG_P^{(+)}V\,. \quad (6)$$

In the above equations, $|S_{\vec{k}_{i,f}}\rangle$ is a solution of the unperturbed Hamiltonian H_0 (kinetic energy of the incoming positron plus the target Hamiltonian—$T_{N+1} + H_N$) and is a product of a target state and a plane wave ($|\vec{k}\rangle \otimes |\Phi_i\rangle$); V is the interaction potential between the incident positron and the electrons and nuclei of the target; $\{|\chi_m\rangle\}$ is a set of $(N+1)$-particle functions, which are the product of a N-particle Slater determinant by a one-particle function (configuration state functions, CSFs) that is used to expand the trial scattering wavefunction; $\hat{H} = E - H$ is the total energy of the collision minus the full Hamiltonian of the system, with $H = H_0 + V$; P is a projection operator onto the open-channel space defined by the target eigenfunctions and $G_P^{(+)}$ is the free-particle Green's function projected on the P-space. $Q = (\mathbb{1} - P)$ is the projector onto the closed electronic channels of the target, which are used in the description of polarization effects.

The direct space is constructed considering CSFs of the form

$$|\chi_i\rangle = |\Phi_1\rangle \otimes |\varphi_i\rangle\,, \quad (7)$$

Table 3. Contracted Cartesian Gaussian functions used for oxygen and carbon.

Type	O (exponent)	O (coefficient)	C (exponent)	C (coefficient)
s	7816.540	0.006 436	4232.610	0.006 228
s	1175.820	0.048 924	634.8820	0.047 676
s	273.1880	0.233 819	146.0970	0.231 439
s	81.169 60	0.784 798	42.497 40	0.789 108
s	27.183 60	0.803 381	14.189 20	0.791 751
s	3.413 600	0.316 720	1.966 600	0.321 870
s	9.532 200	1.000 000	5.147 700	1.000 000
s	0.939 800	1.000 000	0.496 200	1.000 000
s	0.284 600	1.000 000	0.153 300	1.000 000
s	0.065 000	1.000 000	0.050 000	1.000 000
s	0.026 000	1.000 000	0.020 000	1.000 000
s	0.013 000	1.000 000	0.010 000	1.000 000
s	0.005 200	1.000 000	0.004 000	1.000 000
p	35.183 20	0.040 023	18.155 70	0.039 196
p	7.904 000	0.253 849	3.986 400	0.244 144
p	2.305 100	0.806 842	1.142 900	0.816 775
p	0.717 100	1.000 000	0.359 400	1.000 000
p	0.213 700	1.000 000	0.114 600	1.000 000
p	0.080 000	1.000 000	0.050 000	1.000 000
p	0.026 000	1.000 000	0.020 000	1.000 000
p	0.009 100	1.000 000	0.007 000	1.000 000
d	1.426 000	1.000 000	1.097 000	1.000 000
d	0.413 400	1.000 000	0.318 000	1.000 000
d	0.117 000	1.000 000	0.090 000	1.000 000

where $|\Phi_1\rangle$ is an N-electron Slater determinant of the target ground state obtained at the Hartree–Fock level and $|\varphi_i\rangle$ is a one-particle function which represents the incoming positron. These one-particle functions composing the set are used as scattering orbitals.

To take polarization effects into account, the direct space is enlarged by considering CSFs from the closed-channel space, which are constructed as

$$|\chi_{ij}\rangle = |\Phi_i\rangle \otimes |\varphi_j\rangle \,, \tag{8}$$

where $|\chi_{ij}\rangle$ is an N-particle Slater determinant and is obtained by performing single (virtual) excitations from the occupied molecular (hole) orbitals to a set of unoccupied molecular (particle) orbitals. $|\varphi_j\rangle$ is again a one-particle function used as a scattering orbital. The choice of the particle and scattering orbitals will be discussed below.

Our calculations were performed in the static (S) and in the static plus polarization (SP) approximations in the C_{2v} symmetry group. We used the ground-state equilibrium geometry of the molecule as given in [25]. The basis set employed in both bound state and scattering calculations for oxygen, carbon and hydrogen are shown in tables 3 and 4.

As discussed above, to take polarization effects into account, we considered single excitations from the hole (occupied) orbitals to a set of particle (unoccupied) orbitals. We chose improved virtual orbitals (IVOs) [42] to represent the particle and scattering orbitals. In the present calculations, we considered all valence occupied orbitals as hole orbitals and considered excitations to IVOs with energies <2 hartrees to represent the particle and scattering orbitals. With this procedure we obtained 7563 CSFs for A_1 symmetry, 6918 for B_1 symmetry and 5752 for B_2 symmetry. The A_2 symmetry, having a small cross section, was computed in the static exchange approximation.

Table 4. Contracted Cartesian Gaussian functions used for hydrogen.

Type	H (exponent)	H (coefficient)
s	33.865 00	0.025 494
s	5.094 790	0.190 373
s	1.158 790	0.852 161
s	0.325 840	1.000 000
s	0.102 741	1.000 000
s	0.036 000	1.000 000
p	0.750 000	1.000 000

As noted previously, formaldehyde has a permanent electric dipole moment. The calculated dipole moment of the target was 2.85 D, which is in reasonable agreement with the experimental value of 2.43 D [13]. Since the square-integrable basis sets employed in the SMC method cannot account for the long-range dipole interaction, we used a standard Born closure scheme to improve the scattering amplitudes. In short, we computed the scattering amplitude of the dipole potential in the FBA. Then we expanded the scattering amplitude obtained in the SMC method in partial waves up to a chosen value of $\ell_{\rm SMC}$. We also expanded the FBA amplitude of the dipole potential in partial waves. The closure is obtained by keeping the low partial waves (up to $\ell_{\rm SMC}$) computed from the SMC amplitude and adding the high partial waves (from $\ell_{\rm SMC}+1$ to ∞) computed from the FBA dipole amplitude. Details of this procedure have been described in [43]. The choice of $\ell_{\rm SMC}$ was made in order to minimize the difference between the DCSs obtained using the Born closure and the SMC method at high scattering angles. The idea behind this choice is that the low partial waves are well described by the SMC method and the high partial waves are described by the FBA of the dipole potential. In the present calculations, we chose $\ell_{\rm SMC}=1$ from 0.5 to 2.0 eV, $\ell_{\rm SMC}=2$ from 2.5 to 22 eV, $\ell_{\rm SMC}=3$ from 23 to 30 eV, $\ell_{\rm SMC}=4$ from 35 to 45 eV and $\ell_{\rm SMC}=5$ at 50 eV.

4. Results and discussion

In table 1 and figure 2, we present the results of our positron-CH_2O TCS measurements. Note that the errors listed in table 1 and plotted in figure 2 are purely statistical and are at the one standard deviation level. Further note that the arrows in figure 2 indicate, respectively, the approximate thresholds for positronium formation (Ps) and the direct (first) ionization potential (IP) in formaldehyde. It is known [44, 45] that the first IP of CH_2O has a value of ~10.87 eV [44], leading to a positronium threshold value of 4.07 eV as in general:

$$E_{\rm Ps} = {\rm IP} - 6.8\ {\rm eV}. \tag{9}$$

A close examination of the experimental points in figure 2 suggests the existence of a change in slope at about 4 eV, possibly corresponding to the opening of the positronium channel. In figure 2, we also plot our SMC-S + Born and SMC-SP + Born integral elastic cross sections for positron scattering. These data are tabulated in table 5. Finally, the current TCS results for electron-CH_2O scattering from our

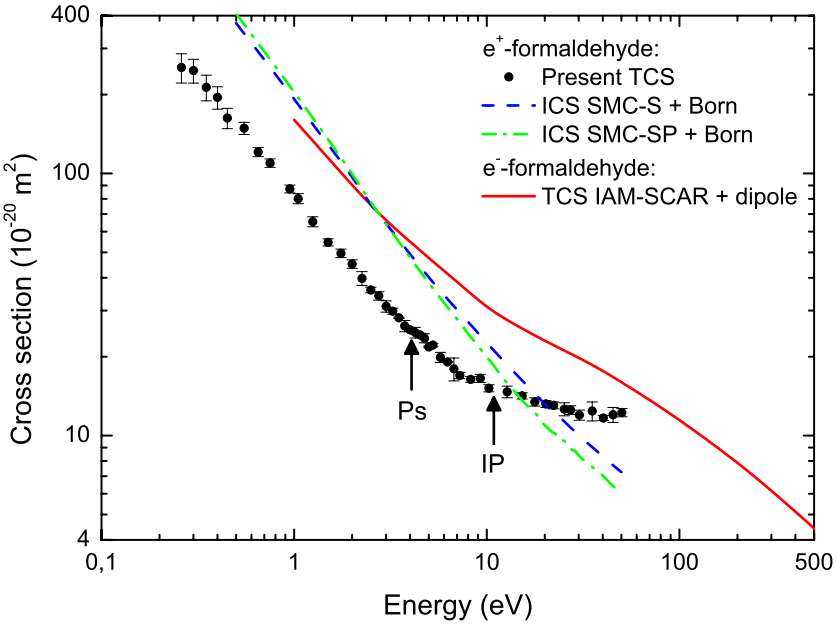

Figure 2. Present experimental (•) TCSs and theoretical elastic ICSs at the SMC-S + Born (– – –) and SMC-SP + Born (– · –) levels for positron-CH_2O scattering. The positronium formation threshold and the first ionization potential are indicated by arrows labelled 'Ps' and 'IP'. Also plotted are our electron scattering TCSs within the IAM-SCAR + dipole (—) formalism.

IAM-SCAR + dipole method are listed in table 2 and plotted in figure 2.

Let us start by looking at the positron results, where it is clear (see figure 2) that as we go to lower positron energies, the magnitude of the experimental TCS and the magnitude of both SMC-level elastic ICSs increase significantly (note the log scale on the *y*-axis). From the experimental perspective, this magnitude is even more significant when one considers the following two factors. First, with an energy resolution of ∼0.26 eV (FWHM), our lowest energy TCSs ($\lesssim$0.5 eV) are actually a convolution over this energy width. In practice, this implies that should the TCSs be corrected for this effect, they would somewhat further increase in magnitude. Secondly, as noted in section 2, the data in table 1 are not corrected for forward angle scattering effects. Makochekanwa *et al* [46], using theoretical elastic DCSs, demonstrated that in water at 0.5 eV the TCS measured with their apparatus should be increased by ∼67% and at 5 eV by ∼53% to account for this effect. Similarly, now with formic acid, a 45% increase in their TCS for this effect at 4 eV positron energy was calculated. As CH_2O has a significantly larger dipole moment than either water or formic acid, it is reasonable to assume that this effect might even be more severe in CH_2O. Note that at higher positron energies, Makochekanwa *et al* [46] found that this correction was not nearly as significant as at the lower energies. Further discussion of this point can be found in Sullivan *et al* [28]. Of course we could use the present SMC-level elastic DCSs, in a similar manner to that in [46], to make corrections to our TCS data for this angular discrimination effect. However, as we discuss in more detail below, as we have only qualitative accord between our measured and calculated TCS/ICS results, such a correction would be a little premature at this time.

It is clear from figure 2 that, below the positronium formation energy, there is good qualitative (shape) accord between our measured TCS and calculated elastic ICS. Above E_{Ps}, we would not expect a good correspondence between them, as the present SMC calculations do not account for positronium formation, direct ionization and the opening of the many valence and Rydberg electronic states that formaldehyde is known to possess [47]. Note that including such channels would not only be very difficult, particularly for positronium which is inherently multi-centred, but also computationally expensive. As a consequence, we focus our discussion on energies less than E_{Ps}. We begin by noting that of course it is unphysical for an elastic ICS to be greater in magnitude than the corresponding TCS (see figure 2). We believe that there are three possible causes for this observation, all of which might be making a contribution. First, as discussed in detail above, the experimental TCSs are not corrected for the instrumental forward angle scattering and finite energy-resolution convolution effects. Second, we note that in the experiment, the formaldehyde sample exists in a distribution of allowed rotational states (J), given by the Boltzmann distribution, whereas the positron computation is for scattering from only $J = 0$. Finally, it is well known [48] that the Born closure approach generally overestimates the lower energy values of the elastic ICS, as the corresponding DCS diverges in the very forward angle direction. Concentrating now on our SMC-level results, we see that while polarization is playing a role (compare the SMC-SP + Born magnitudes to the SMC-S + Born magnitudes in figure 2 for $E < E_{Ps}$) in the scattering dynamics, it is not as significant as we had previously seen in our study on formic acid [12]. On the other hand, if we were to 'turn off' the Born-closure correction, the magnitude of the elastic ICS would drop significantly (not shown in figure 2). This observation highlights the crucial, perhaps predominant, role that the target molecular dipole moment plays in the low-energy scattering dynamics of this system. Finally, we observe

Table 5. The present calculated elastic ICS ($\times 10^{-20}$ m^2) for positron scattering from formaldehyde, using our SMC-S + Born and SMC-SP + Born methods.

Energy	SMC-S + Born	SMC-SP + Born
0.5	374.50	407.08
1.0	192.10	205.37
1.5	128.90	135.11
2.0	96.87	100.01
2.5	76.27	77.42
3.0	64.44	64.29
3.5	55.79	54.82
4.0	49.24	47.75
4.5	44.17	42.37
5.0	40.18	38.23
5.5	36.98	34.84
6.0	34.36	32.09
6.5	32.16	29.82
7.0	30.26	27.85
7.5	28.60	26.14
8.0	27.13	24.41
8.5	25.81	23.21
9.0	24.63	21.93
9.5	23.57	20.92
10.0	22.60	19.94
11.0	20.94	18.31
12.0	19.54	16.75
13.0	18.36	15.59
14.0	17.33	14.67
15.0	16.44	13.82
16.0	15.65	13.14
17.0	14.94	12.55
18.0	14.30	12.24
19.0	13.72	11.30
20.0	13.19	10.79
21.0	12.71	10.61
22.0	12.26	10.23
23.0	12.09	10.17
24.0	11.73	9.58
25.0	11.40	9.64
26.0	11.09	9.30
27.0	10.80	8.99
28.0	10.53	8.76
29.0	10.27	8.75
30.0	10.03	8.33
35.0	9.08	7.62
40.0	8.34	7.09
45.0	7.73	6.38
50.0	7.25	6.11

in figure 2 that the magnitude of our SMC-SP + Born elastic ICS drops below that of our SMC-S + Born elastic ICS at an energy very close to that for the opening of the positronium formation channel. While this might well be coincidental, it is curious nonetheless, as there is ample evidence [49] linking the magnitude of the target dipole polarizability (which in some sense is a measure for the extent of the molecular electron charge cloud) to the strength of positronium formation.

Comparing now our measured (positron) and calculated (electron) TCSs (again see figure 2) we observe that there is a qualitative correspondence between them at lower energies, i.e. a similar energy dependence for both leptons. Indeed, we are confident that this correspondence would become even more transparent once the forward angle scattering corrections are applied to the measured positron data. At higher energies, the present positron TCSs appear to be trending towards our calculated electron TCSs, perhaps converging at around 100 eV. This we believe is physical, as the two most important phenomenological differences between them—exchange in the case of the incident electrons and positronium formation in the case of the incident positrons—typically become small at incident projectile energies above 100 eV.

5. Conclusions

We have reported results from a joint theoretical and experimental study into positron and electron scattering from formaldehyde. Good qualitative (shape) agreement between our measured positron TCSs and SMC calculated elastic ICSs, particularly below the opening of the positronium formation channel, was found. This comparison also highlighted the important role played by the permanent dipole moment of CH_2O in the scattering process. The experimental results also clearly indicated the importance of the opening of the positronium formation channel on the reaction. The present positron TCSs were found to trend towards our calculated electron TCSs, perhaps converging at around 100 eV where the effects of exchange, in the electron case, and positronium formation, in the positron case, become small. The present study also highlighted the need for some experimental electron-CH_2O TCSs to be measured.

Acknowledgments

This work was supported under a Memorandum of Understanding between the University of Trento and the Flinders University node of the ARC Centre of Excellence for Antimatter-Matter Studies. GG and FB thank the Spanish Ministerio de Ciencia e Innovacion (project FIS2009-10245), while GG, FB and MJB acknowledge the EU Framework Programme (Cost Actions MP1002 and CM0601). MJB also thanks the University of Malaya for his 'Visiting Distinguished Professor' appointment. MHFB, MT do NV and MAPL acknowledge support from the Brazilian agency Conselho Nacional de Desenvolvimento Científico e Tecnológico (CNPq). MHFB acknowledges support from FINEP (under Project no CT-Infra). MT do NV and MAPL acknowledge support from FAPESP. MHFB also acknowledges computational support from Professor Carlos M de Carvalho at DFis-UFPR and LCPAD-UFPR. The authors acknowledge computational support from CENAPAD–SP. The authors also thank Dr L Campbell for his help in producing this manuscript, and Mr Andrea Defant for his advice on how to obtain a pure formaldehyde vapour.

References

[1] Bode B M and Gordon M S 1998 *J. Mol. Graph. Model.* **16** 133
[2] Zecca A, Sanyal D, Chakrabarti M and Brunger M J 2006 *J. Phys. B: At. Mol. Opt. Phys.* **39** 1597
[3] Zecca A, Perazzolli C and Brunger M J 2005 *J. Phys. B: At. Mol. Opt. Phys.* **38** 2079
[4] Zecca A, Chiari L, Sarkar A and Brunger M J 2008 *J. Phys. B: At. Mol. Opt. Phys.* **41** 085201

[5] Zecca A, Chiari L, Trainotti E, Sarkar A and Brunger M J 2010 *PMC Phys.* B **3** 4
[6] Zecca A, Chiari L, Garcia G, Blanco F, Trainotti E and Brunger M J 2010 *J. Phys. B: At. Mol. Opt. Phys.* **43** 215204
[7] Zecca A, Chiari L, Garcia G, Blanco F, Trainotti E and Brunger M J 2011 *New J. Phys.* **13** 063019
[8] Fuss M C, Muñoz A, Oller J C, Blanco F, Hubin-Franskin M-J, Almeida D, Limão-Vieira P and García G 2010 *Chem. Phys. Lett.* **486** 110
[9] Muñoz A, Blanco F, García G, Thorn P A, Brunger M J, Sullivan J P and Buckman S J 2008 *Int. J. Mass Spectrom.* **277** 175
[10] Šuvakov M, Petrović Z Lj, Marler J P, Buckman S J, Robson R E and Malović G 2008 *New J. Phys.* **10** 053034
[11] Marler J P, Petrović Z Lj, Banković A, Dujko S, Šuvakov M, Malović G and Buckman S J 2009 *Phys. Plasmas* **16** 057101
[12] Zecca A, Chiari L, Sarkar A, Lima M A P, Bettega M H F, Nixon K L and Brunger M J 2008 *Phys. Rev.* A **78** 042707
[13] Schoolery J N and Sharbaugh A H 1951 *Phys. Rev.* **82** 95
[14] Applequist J, Carl J R and Fung K-K 1972 *J. Am. Chem. Soc.* **94** 2952
[15] Freitas T C, Lima M A P, Canuto S and Bettega M H F 2009 *Phys. Rev.* A **80** 062710
[16] Kaur S and Baluja K L 2005 *J. Phys. B: At. Mol. Opt. Phys.* **38** 3917
[17] Rescigno T N, McCurdy C W and Schneider B I 1989 *Phys. Rev. Lett.* **63** 248
[18] Benoit C, Abouaf R and Cvejanovic S 1987 *Chem. Phys.* **117** 295
[19] Chutjian A 1974 *J. Chem. Phys.* **61** 4279
[20] Kato H, Makochekanwa C, Hoshino M, Kimura M, Cho H, Kume T, Yamamoto A and Tanaka H 2006 *Chem. Phys. Lett.* **425** 1
[21] Zecca A, Chiari L, Sarkar A and Brunger M J 2011 *New J. Phys.* at press
[22] Zecca A, Chiari L, Sarkar A, Chattopadhyay S and Brunger M J 2010 *Nucl. Instrum. Methods* B **268** 533
[23] Jones A C L *et al* 2011 *Phys. Rev.* A **83** 032701
[24] Makochekanwa C *et al* 2011 *Phys. Rev.* A **83** 032721
[25] Lide D R (ed) 1998 *CRC Handbook of Chemistry and Physics* 79th edn (Boca Raton, FL: CRC Press)
[26] Kauppila W E, Stein T S, Smart J H, Dababneh M S, Ho Y K, Downing J P and Pol V 1981 *Phys. Rev.* A **24** 725
[27] Hamada A and Sueoka O 1994 *J. Phys. B: At. Mol. Opt. Phys.* **27** 5055
[28] Sullivan J P, Makochekanwa C, Jones A, Caradonna P, Slaughter D S, Machacek J, McEachran R P, Mueller D W and Buckman S J 2011 *J. Phys. B: At. Mol. Opt. Phys.* **44** 035201
[29] Zecca A and Brunger M J 2007 *Nanoscale Interactions and Their Applications: Essays in Hounour of Ian M^{c}Carthy* ed F Wang and M J Brunger (Trivandrum, India: Research Signpost)
[30] Takaishi T and Sensui Y 1963 *Trans. Faraday Soc.* **59** 2503
[31] Riley M E and Truhlar D G 1975 *J. Chem. Phys.* **63** 2182
[32] Zhang X Z, Sun J F and Liu Y F 1992 *J. Phys. B: At. Mol. Opt. Phys.* **25** 1893
[33] Staszewska G, Schwenke D W, Thirumalai D and Truhlar D G 1983 *Phys. Rev.* A **28** 2740
[34] Zatsarinny O *et al* 2011 *Phys. Rev.* A **83** 042702
[35] Blanco F and Garcia G 2004 *Phys. Lett.* A **330** 230
[36] Blanco F and García G 2009 *J. Phys. B: At. Mol. Opt. Phys.* **42** 145203
[37] Hargreaves L R, Brunton J R, Prajapati A, Hoshino M, Blanco F, García G, Buckman S J and Brunger M J 2011 *J. Phys. B: At. Mol. Opt. Phys.* **44** 045207
[38] Germano J S E and Lima M A P 1993 *Phys. Rev.* A **47** 3976
[39] da Silva E P, Germano J S E and Lima M A P 1994 *Phys. Rev.* A **49** R1527
[40] da Silva E P, Germano J S E and Lima M A P 1996 *Phys. Rev. Lett.* **77** 1028
[41] da Silva E P, Germano J S E, Lino J L S, de Carvalho C R C, Natalense A P P and Lima M A P 1998 *Nucl. Instrum. Methods Phys. Res.* B **143** 140
[42] Hunt W J and Goddard III W A 1969 *Chem. Phys. Lett.* **3** 414
[43] Khakoo M A *et al* 2008 *Phys. Rev.* A **77** 042705
[44] Guyon P M, Chupka W A and Berkowitz J 1976 *J. Chem. Phys.* **64** 1419
[45] Domcke W and Cederbaum L S 1976 *J. Chem. Phys.* **64** 612
[46] Makochekanwa C *et al* 2009 *New J. Phys.* **11** 103036
[47] Weiss M J, Kuyatt C E and Mielczarek S 1971 *J. Chem. Phys.* **54** 4147
[48] Bouchiha D, Gorfinkiel J D, Caron L G and Sanche L 2007 *J. Phys. B: At. Mol. Opt. Phys.* **40** 1259
[49] Chiari L, Brunger M J and Zecca A 2011 *Radiation Damage in Biomolecular Systems* ed M C Fuss and G García (Berlin: Springer)